THE JOURNAL OF BIOLOGICAL CHEMISTRY VOL. 290, NO. 3, pp. 1760–1769, January 16, 2015
© 2015 by The American Society for Biochemistry and Molecular Biology, Inc. Published in the U.S.A.

Interhelical Interaction and Receptor Phosphorylation Regulate the Activation Kinetics of Different Human β_1-Adrenoceptor Variants

Received for publication, August 26, 2014, and in revised form, November 25, 2014 Published, JBC Papers in Press, December 1, 2014, DOI 10.1074/jbc.M114.607333

Andrea Ahles[‡], **Fabian Rodewald**[‡], **Francesca Rochais**[§1], **Moritz Bünemann**[¶], **and Stefan Engelhardt**[‡‖2]

From the [‡]*Institute of Pharmacology and Toxicology, Technische Universität München, 80802 Munich, Germany, the* [§]*Rudolf Virchow Center for Experimental Biomedicine, Universität Würzburg, 97080 Würzburg, Germany, the* [¶]*Institute of Pharmacology and Clinical Pharmacy, Universität Marburg, 35043 Marburg, Germany, and the* [‖]*German Center for Cardiovascular Research, Partner Site Munich Heart Alliance, 80802 Munich, Germany*

Background: The mechanism underlying the hyperfunctionality of the Arg-389 variant of the human β_1-adrenoceptor is elusive.
Results: Real-time FRET imaging of the Arg-389 variant in combination with site-directed mutagenesis revealed faster activation kinetics compared with the hypofunctional Gly-389 variant.
Conclusion: Interhelical interaction of Arg-389 regulates receptor activation speed and efficacy.
Significance: Our findings deepen the understanding of heterogeneity of drug responses observed for the β_1-adrenoceptor.

G protein-coupled receptors represent the largest class of drug targets, but genetic variation within G protein-coupled receptors leads to variable drug responses and, thereby, compromises their therapeutic application. One of the most intensely studied examples is a hyperfunctional variant of the human β_1-adrenoceptor that carries an arginine at position 389 in helix 8 (Arg-389-ADRB1). However, the mechanism underlying the higher efficacy of the Arg-389 variant remained unclear to date. Despite its hyperfunctionality, we found the Arg-389 variant of ADRB1 to be hyperphosphorylated upon continuous stimulation with norepinephrine compared with the Gly-389 variant. Using ADRB1 sensors to monitor activation kinetics by fluorescence resonance energy transfer, Arg-389-ADRB1 exerted faster activation speed and arrestin recruitment than the Gly-389 variant. Both activation speed and arrestin recruitment depended on phosphorylation of the receptor, as shown by knockdown of G protein-coupled receptor kinases and phosphorylation-deficient ADRB1 mutants. Structural modeling of the human β_1-adrenoceptor suggested interaction of the side chain of Arg-389 with opposing amino acid residues in helix 1. Site-directed mutagenesis of Lys-85 and Thr-86 in helix 1 revealed that this interaction indeed determined ADRB1 activation kinetics. Taken together, these findings indicate that differences in interhelical interaction regulate the different activation speed and efficacy of ADRB1 variants.

The β_1-adrenoceptor (ADRB1) is a G protein-coupled receptor (GPCR)[3] that transduces sympathetic stimulation and catecholamine release into cellular responses (1). It serves a key role in the autonomic nervous system control of various organ functions as well as in various disease states. Consequently, both agonists and antagonists at ADRB1 (*i.e.* β-agonists and β-blockers) are in clinical use, and the latter have evolved as one of the most effective and widely used classes of drugs (2). The efficacy of ADRB1 signaling and the response to β-blockers has been reported to vary among patients, and this has been attributed to sequence variation within the coding sequence of *ADRB1* (3). Multiple association studies have identified c.1165C>G as the most relevant among the variants in *ADRB1* (4). This variant is the most common non-synonymous variation in the *ADRB1* gene and results in an amino acid substitution from arginine to glycine at position 389 in the ADRB1 protein. p.Arg389Gly is located in amphiphilic helix 8, which is formed by a stretch of amino acids starting from the distal seventh transmembrane-spanning domain to the membrane-anchoring palmitoylated cysteine. Its minor allelic frequency (*i.e.* the frequency of the codon for Gly-389) is approximately 27% in Caucasians and about 42% in African Americans (5, 6). The Arg-389 variant has been identified as hyperfunctional with a higher efficacy toward cAMP formation (5, 7, 8). Also, the sensitivity of receptor conformational changes for the β-blocker carvedilol was enhanced for the Arg-389 variant (9). In line with hyperfunctionality of Arg-389-ADRB1, it has been associated with higher blood pressure in large candidate gene studies (10–12). Moreover, stronger responses to β-agonists in healthy individuals and to β-blocker treatment in cohorts of heart failure patients have been reported for the Arg-389 variant (4). Despite the well established functional importance of the ADRB1 variation at position 389, the mechanistic basis of the altered efficacy of ADRB1 variants remained unclear. Recently developed approaches allow the rapid monitoring of GPCR activation in living cells (9, 13–15). In a previous study, we monitored activation of the β_2-adrenoceptor and demonstrated that this GPCR rapidly changes its original activation kinetics after initial agonist stimulation (13).

[1] Present address: Developmental Biology Institute, Université de la Méditerranée, 13288 Marseille, France.
[2] To whom correspondence should be addressed: Institute of Pharmacology and Toxicology, Technische Universität München, Biedersteiner Str. 29, 80802 Munich, Germany. Tel.: 49-89-4140-3260; Fax: 49-89-4140-3261; E-mail: stefan.engelhardt@tum.de.
[3] The abbreviations used are: GPCR, G protein-coupled receptor; Cer, Cerulean; NE, norepinephrine; GRK, G protein-coupled receptor kinase; RFP, red fluorescent protein; YFP, yellow fluorescent protein.

Here we use FRET sensors for the ADRB1 variants Arg-389 and Gly-389 to monitor their activation. We show that the Arg-389-ADRB1 is hyperphosphorylated and that this determines its activation speed and arrestin recruitment. Structural modeling followed by site-directed mutagenesis of human ADRB1 further revealed that interaction of the guanidinium group of Arg-389 with opposing amino acid residues in helix 1 regulates its higher activation speed. Our findings propose a molecular mechanism by which a common variant in human ADRB1 determines receptor function.

EXPERIMENTAL PROCEDURES

Molecular Biology and Cell Culture—The generation of the ADRB1-FRET sensors for both the Arg-389 and the Gly-389 variant has been described previously (9). eYFP-F46L was inserted into the third intracellular loop of the receptor at amino acid position 273 (NotI restriction site). The Cerulean variant of GFP was ligated to the carboxyl terminus of the human ADRB1 sequence separated by a linker of five glycine residues (in the sensor constructs and the single-labeled ADRB1-Cer constructs). A receptor C terminus with all serines and threonines exchanged to alanine was synthetized by Genescript and was used to create phosphorylation-deficient ADRB1 constructs. Point mutations at amino acid position 85 (Lys → Leu) and 86 (Thr → Val) in transmembrane helix 1 were introduced by PCR amplification of the fragments upstream and downstream of the respective sequence using Accu Pfx DNA polymerase and primers that carried the desired mutation (Leu codon TTG, Val codon GTG). The fragments were then merged by PCR, and the wild-type sequence in the sensor constructs was replaced by the mutated fragment by conventional ligation with T4 ligase (New England Biolabs). ARRB2 was amplified from cDNA of HEK293 cells and N-terminally tagged with eYFP-F46L separated by a 5× Gly linker.

All constructs were verified by sequencing and subcloned into the vector pT-Rex DEST30 (Invitrogen) for expression in HEK293 cells. The Effectene transfection reagent from Qiagen was used to transiently or stably express the respective constructs in HEK293 cells. HEK293 cells were cultured in DMEM (Invitrogen) supplemented with 10% FBS (PAN), 100 units/ml penicillin, and 0.1 mg/ml streptomycin (Invitrogen) at 37 °C in a 5% CO_2 atmosphere. Cells lines that stably expressed the polymorphic receptor or sensor variants were selected in the presence of G-418 (Invitrogen, 0.4–0.8 mg/ml) and characterized in radioligand-binding assays.

siRNA-mediated Knockdown of GRKs—Synthetic siRNA duplexes were purchased from Sigma-Aldrich for the following mRNA targets: GRK2 (5′-GAAAUUCAUUGAGAGCGAU-3′), GRK3 (5′-CAGUUUAUGAAGCAGUAAA-3′), GRK5 (5′-GCAGUAUCGAGUGCUAGGA-3′), and GRK6 (5′-CACCUUCAGGCAAUACCGA-3′). A scrambled RNA duplex (5′-GCUUAGGAGCAUUAGUAAA-3′) served as a negative control. HEK293 cells were transfected with 200 nM of each siRNA duplex using HiPerFect (Qiagen) according to the protocol of the manufacturer. After 48 h, the cells were split onto coverslips for FRET measurements performed 24 h later. Successful knockdown was verified by Western blotting 72 h after transfection.

Membrane Preparation and Radioligand-binding Assays—HEK293 cells stably expressing the ADRB1 (sensor) variants (and non-transfected control cells) were grown in cell culture dishes to a confluency of about 70%, washed twice with PBS, and frozen at −20 °C. After thawing, the cells were resuspended in hypotonic buffer (5 mM Tris-HCl and 2 mM EDTA (pH 7.4)), homogenized, and centrifuged twice, first at 1400 × *g* to remove nuclei and cell debris and finally at 80,000 × *g* to obtain the crude membrane fraction as the pellet, which was then resuspended in hypotonic buffer. Protein content was determined using the Bradford method with bovine serum albumin Bradford method with bovine serum albumin (Sigma-Aldrich) as a standard or with the BCA protein assay kit (Thermo Scientific).

Radioligand-binding experiments were performed in a volume of 200 μl in 50 mM Tris-HCl (pH 7.4) (assay buffer) with 10 μg of membrane protein in the presence of 100 μM GTP (Sigma-Aldrich) to ensure monophasic binding curves. Nonspecific binding was determined in the presence of 10 μM alprenolol (Sigma-Aldrich). For saturation binding experiments, we used 1 nM [^{3}H]CGP-12177 (Hartmann Analytic).

Incubation was carried out at room temperature for 2 h. Subsequently, the protein was transferred onto Printes Filtermat A glass fiber filters using a Filter Mate Harvester (PerkinElmer Life Sciences). After 1 h at 42 °C, the filter was sealed with MeltiLex A melt-on scintillator sheets in a Wallac 1495-021 microsealer (PerkinElmer Life Sciences), and the bound radioactivity was counted in a 1450 MicroBeta TriLux microplate scintillation and luminescence counter and recorded by a MicroBeta Windows workstation.

For expression analysis of the wild-type ADRB1 sensor variants, membrane fractions were incubated for 90 min at 30 °C with 50 pM [^{125}I]cyanopindolol and different concentrations of norepinephrine, filtered through Whatman GF/C filters, and washed three times with ice-cold assay buffer. Samples were counted in a γ counter (Wallac 1480 Wizard 3″). IC_{50} values were calculated using Prism 5.0b (GraphPad) and transformed into K_i values according to the equation of Cheng and Prusoff (34).

Radioligand-binding on intact cells was performed in HEK293 cells stably expressing the ADRB1 variants and seeded in 24-well plates precoated with poly-D-lysine (Sigma-Aldrich). Cells were incubated for 90 min with different concentrations of norepinephrine (Sigma-Aldrich) in the presence of 1 nM [^{3}H]CGP-12177 (Hartmann Analytic) in serum-free DMEM.

FRET Measurements—HEK293 cells stably expressing the ADRB1 sensor variants or HEK293 cells transiently transfected with ADRB1-Cer and YFP-ARRB2 24 h earlier were seeded on poly-D-lysine-coated coverslips in DMEM containing 10% FBS and used for FRET experiments the day after. During the experiment, cells were maintained at room temperature in assay buffer (140 mM NaCl, 4.5 mM KCl, 10 mM Hepes, 2 mM $CaCl_2$, and 2 mM $MgCl_2$ (pH 7.3)). A stock solution of 100 mM (−)-norepinephrine (Sigma-Aldrich) was prepared in double-distilled H_2O. FRET experiments were performed with a Zeiss Axio Observer Z1 inverted microscope equipped with an oil immersion ×100 objective. A Polychrome 5000 (TILL Photonics) served as monochromatic light source to excite Cer at 436 ± 15 nm and YFP at 490 ± 15 nm. FRET was monitored as the emission ratio of YFP to Cer,

F_{535}/F_{436}, with F_{535} and F_{480} displaying the emission intensities at 535 ± 15 nm and 480 ± 20 nm, respectively (T495LP dichroic beam splitter) upon excitation at 436 nm (455 nm dichroic longpass (DLCP) beam splitter).

Receptor activation was recorded using a dual emission photometric system (TILL Photonics). The illumination time was set to ≤50 ms with a frequency of 10 Hz (40 Hz for kinetics). The signals detected by the photodiodes were digitalized with an analog digitizer converter (Digidata 1440A, Axon Instruments), recorded with Clampex 10.2 (Axon Instruments), and analyzed with Clampfit 10.2 (Axon Instruments) and Origin 6.1 (OriginLab). The receptor-arrestin interaction was detected via DualView2 and an Evolve camera (Photometrics). FRET was monitored with Metafluor software (Molecular Devices) and analyzed with Origin 6.1 (OriginLab). The emission ratio was corrected for spillover of Cer into the 535-nm channel and for direct excitation of YFP at 436 nm. For the ADRB1-ARRB2 interaction analysis, cells with a comparable expression ratio of ADRB1-Cer/YFP-ARRB2 were selected.

For monitoring stimulation-induced changes in FRET, cells were continuously superfused with assay buffer, and the ligand was applied with a computer-assisted solenoid valve-controlled rapid superfusion device system (ALA VC3-8, ALA Scientific Instruments). Repeated stimulation was carried out after complete washout of the agonist of the earlier stimulation.

For permeabilization, cells attached to poly-D-lysine-coated coverslips were incubated with internal buffer (100 mM K^+ aspartate, 30 mM KCl, 10 mM NaCl, 1 mM $MgCl_2$, 5 mM EGTA, and 10 mM Hepes (pH 7.35)) containing 0.05% saponin (Sigma-Aldrich) for 3 min at room temperature and subsequently superfused with internal buffer with or without (−)-norepinephrine for the FRET experiments.

Confocal Microscopy—Three systems were used for confocal analysis: a Leica TCS SP2 system equipped with a ×63 oil objective, an argon laser for excitation of YFP (514-nm laser line), and a diode laser for excitation of Cer at 430 nm (the factory settings were used for recording of the images); an Olympus Konfokal FV1000 system equipped with a ×100 water objective and lasers for excitation of YFP (515 nm), Cer (430 nm), and RFP (559 nm); and a Leica TCS SP5II system equipped with a ×63 oil objective, an UV laser for excitation of Cer (405 nm), and an argon laser for excitation of YFP (515 nm).

Assessment of cAMP Formation—HEK293 cells stably expressing the polymorphic ADRB1 variants were seeded in 384-well plates, starved overnight, and stimulated with NE for the respective times. cAMP was quantified with the cAMP dynamic 2 kit (Cisbio Bioassays) following the "two-step protocol" of the manufacturer and detected in a homogeneous time resolved fluorescence (HTRF) Pherastar FS reader (BMG Biotech).

Biochemical Assays—For Western blot analysis, cells were washed once with ice-cold PBS and lysed directly on ice in buffer containing 50 mM Tris (pH 6.7), 2% SDS, 1 mM Na_3VO_4, and protease inhibitor (Complete Mini from Roche or Halt protease inhibitor mixture from Thermo Scientific). Proteins were quantified using the Pierce BCA protein assay kit (Thermo Scientific). 5–20 μg were separated by SDS-PAGE in gels containing 10 or 12% acrylamide and transferred onto Immobilion-P membranes (Millipore Corp.). After blocking the membranes with 5% milk powder for 2 h at room temperature, they were incubated with primary antibody overnight at 4 °C (GRK2, catalog no. sc-562, 1:1000; GRK3, catalog no. sc-563, 1:1000; GRK5, catalog no. sc-565, 1:500; GRK6, catalog no. sc-566, 1:1000; and HSP90, catalog no. sc-13119, 1:5000; Santa Cruz Biotechnology). Incubation with goat anti-mouse or anti-rabbit secondary antibody (Dianova, 1:10,000) was carried out after washing the membranes in PBS supplemented with 0.1% Tween 20. Chemiluminescent detection was achieved in a LAS-mini4000 (Bio-Rad) using the ECL or ECL-Plus detection system from Thermo Scientific. Blots were processed and quantified using Multi Gauge software (Fujifilm).

To assess phosphorylation of ADRB1 in intact cells, stably transfected HEK293 cells overexpressing the polymorphic variants were seeded in 12-well plates in phosphate-free DMEM. The following day, the cells were labeled with 30 μCi/well of [^{32}P]orthophosphate (Hartmann Analytic) in phosphate-free DMEM for 4 h and then stimulated at 37 °C as indicated. After washing once with ice-cold PBS, cell lysis was achieved by addition of radioimmune precipitation assay (RIPA) buffer (1% Nonidet P-40, 0.5% sodium deoxycholate, 0.1% SDS, 50 mM Tris (pH 7.4), 100 mM NaCl, and 2 mM EDTA) supplemented with Halt phosphatase and protease inhibitor mixtures (Thermo Scientific) and incubation on ice for 30 min. After centrifugation for 10 min, ADRB1 was immunoprecipitated out of the resulting protein supernatant with 2 μg of anti-ADRB1 antibody (a gift from M. Ungerer, advanceCOR) and 1 mg Dynabeads protein G (Novex). Immunoprecipitated proteins were supplemented with 6× Laemmli buffer, loaded on 10% SDS-polyacrylamide gels, and subsequently blotted onto a PVDF membrane. ^{32}P-labeled proteins were visualized by quantitative filmless autoradiography using a Cyclone Plus PhosphorImager (PerkinElmer Life Sciences) and OptiQuant software (PerkinElmer Life Sciences). The images were exported and quantified with Multi Gauge (Fujifilm).

Statistics—Data are presented as mean ± S.E. Statistical analysis was carried out with the Prism software package (GraphPad, version 6.0c). Student's *t* test and two-way analysis of variance followed by Bonferroni test or corresponding nonparametric tests were used as appropriate. $p < 0.05$ was considered statistically significant.

RESULTS

Enhanced cAMP Formation, Receptor Phosphorylation, and Arrestin Recruitment of Arg-389-ADRB1 Compared with Gly-389-ADRB1—The two variants of the human β_1-adrenoceptor, Arg-389-ADRB1 and Gly-389-ADRB1, were stably expressed in HEK293 cells, and their basic pharmacological properties were assessed. Both receptor variants yielded comparable expression levels (Arg-389-ADRB1, 2.14 ± 0.20 pmol/mg; Gly-389-ADRB1, 2.22 ± 0.15 pmol/mg membrane protein), and the binding affinity for the endogenous agonist norepinephrine (NE) was determined by radioligand-binding with CGP-12177 on intact cells (Arg-389-ADRB1, $K_i = 4.2 \pm 0.3$ μM; Gly-389-ADRB1, $K_i = 4.3 \pm 0.3$ μM; $n = 5–6$). We next sought to address the efficacy of the two ADRB1 variants to promote formation of the second messenger cAMP. Stimulation with NE for 10 min yielded a 67% higher efficacy of Arg-389-ADRB1 with regard to cAMP formation compared with

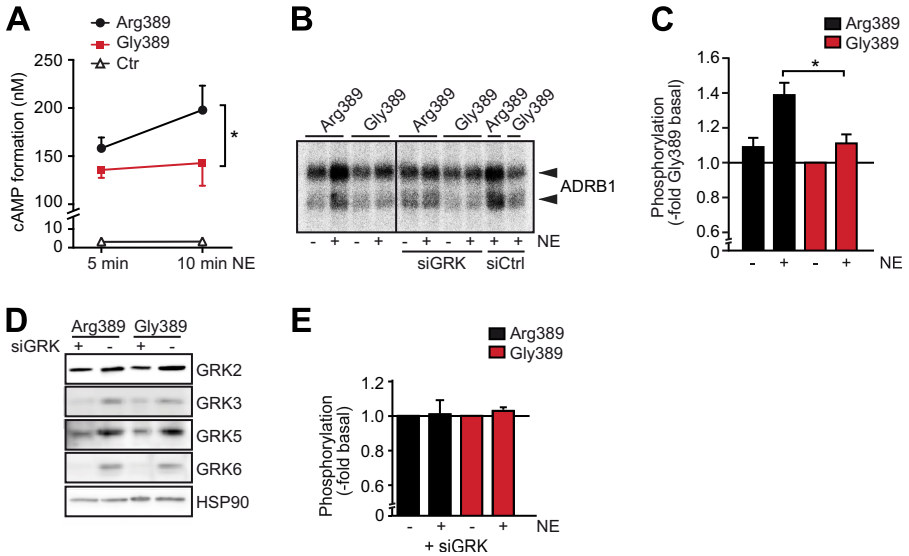

FIGURE 1. **The Arg-389 variant of the β_1-adrenoceptor is hyperfunctional with regard to agonist-dependent cAMP formation and hyperphosphorylated.** *A*, cAMP formation in HEK293 cells stably expressing the ADRB1 variants at comparable levels (and non-expressing control (*Ctr*) cells). Stimulation was carried out with 1 μM NE in 384 wells containing 10,000 cells for the indicated time ($n = 4$, with 3–4 replicates each). *, $p < 0.05$; Student's *t* test. *B* and *C*, basal and NE-induced phosphorylation of the ADRB1 variants at position 389. HEK293 cells stably transfected with Arg-389-ADRB1 or Gly-389-ADRB1 were labeled with [^{32}P]orthophosphate. After stimulation with the agonist, the ADRB1 protein was immunoprecipitated, and incorporated radioactivity was quantified by PhosphorImager analysis. *B*, representative PhosphorImager blot (*lanes 5–10*, additional transfection of an siRNA mixture targeting GRK-2, 3, 5, and 6 or a respective scrambled control siRNA). *C*, quantification of phosphorylation of Arg-389-ADRB1 and Gly-389-ADRB1 with and without NE stimulation for 5 min ($n = 5$). *, $p < 0.05$; two-way analysis of variance followed by Bonferroni post test. *D*, representative Western blots of lysates from cells transfected with siRNA targeted against GRK subtypes. *E*, quantification of phosphorylation of Arg-389-ADRB1 and Gly389-ADRB1 with and without NE stimulation for 5 min upon knockdown of GRK-2, 3, 5, and 6 ($n = 3$).

Gly-389-ADRB1 (Fig. 1*A*). Untransfected HEK293 cells showed hardly any increase in cAMP formation upon NE stimulation.

A key regulatory event following β-adrenoceptor activation is the rapid phosphorylation of the receptor protein itself through GRKs. Receptor phosphorylation by GRKs is rapid and promotes binding of β-arrestin, a process that serves both regulatory and signaling functions. We determined the extent of phosphorylation of the two ADRB1 variants by [^{32}P]orthophosphate labeling in stably transfected HEK293 cells. Upon agonist stimulation (100 μM NE, 5 min), ADRB1 was immunoprecipitated from cell lysates, and the precipitate was subjected to gel electrophoresis and blotting to PVDF membranes. Radiographic quantification (Fig. 1*B*) indicated a significantly enhanced agonist-dependent phosphorylation of the Arg-389 variant compared with the Gly-389 variant (Fig. 1*C*). This NE-dependent increase in receptor phosphorylation was primarily dependent on GRKs because it was blunted upon their knockdown by siRNAs (GRKs 2, 3, 5, and 6 in combination; Fig. 1, *D* and *E*). Basal phosphorylation levels were not significantly higher for the Arg-389 variant (Fig. 1*C*). Non-expressing control cells did not show any signal (data not shown).

Because phosphorylation of the β_1-adrenoceptor by GRKs is a prerequisite for its interaction with β-arrestin, we asked whether the observed differences in receptor phosphorylation would determine its interaction with β-arrestin. HEK293 cells were cotransfected with β-arrestin 2 (ARRB2, N-terminally tagged with YFP) and the ADRB1 variants (C-terminally tagged with Cer), and FRET between the two was monitored upon stimulation with NE, indicating the translocation of β-arrestin to the receptor (Fig. 2, *A* and *B*). Both the speed and the amplitude of the change in FRET ratio were significantly higher in Arg-389-ADRB1-expressing cells compared with cells expressing Gly-389-ADRB1 (Fig. 2*C*).

We next investigated whether increased β-arrestin recruitment by Arg-389-ADRB1 required phosphorylation of the receptor C terminus. As expected, mutation of C-terminal putative GRK phosphorylation sites in the ADRB1 protein (Fig. 2*D*) impaired β-arrestin recruitment. Interestingly, the variant-dependent differences both in speed and amplitude of the FRET signal were completely blunted (Fig. 2*E*). The residual agonist-induced change of the FRET ratio might be due to phosphorylation-independent arrestin interaction or to activation-induced exposition of phosphorylated residues in the intracellular loops. Together, these data indicate that Arg-389-ADRB1 is hyperfunctional with regard to cAMP formation and arrestin recruitment and that the latter depends on enhanced phosphorylation of the receptor C terminus.

Arg-389-ADRB1 Exhibits Faster Activation Compared with Gly-389-ADRB1—Previous studies indicated that different ligands (inducing different conformational states) induce differential phosphorylation of the β_2-adrenoceptor C terminus (16) and that receptor phosphorylation determined the activation speed and downstream signaling efficacy of the β_2-adrenoceptor (13). We therefore hypothesized that differences in the kinetics of agonist-promoted receptor conformational changes might account for the observed variant-dependent differences in receptor functionality of ADRB1. We monitored activation of the receptor variants using receptor activation FRET sensors that were stably expressed in HEK293 cells. These sensors allowed the live recording of receptor conformational changes through ligand-induced reorientation of the inserted fluorophores YFP (in the third intracellular loop) and Cerulean (at the C terminus). The sensors localized at the cell surface and retained the pharmacological and functional characteristics of the native ADRB1 variants (Ref. 9 and Fig. 3*A*). Application of the agonist NE led to a decrease in energy transfer from Cer to

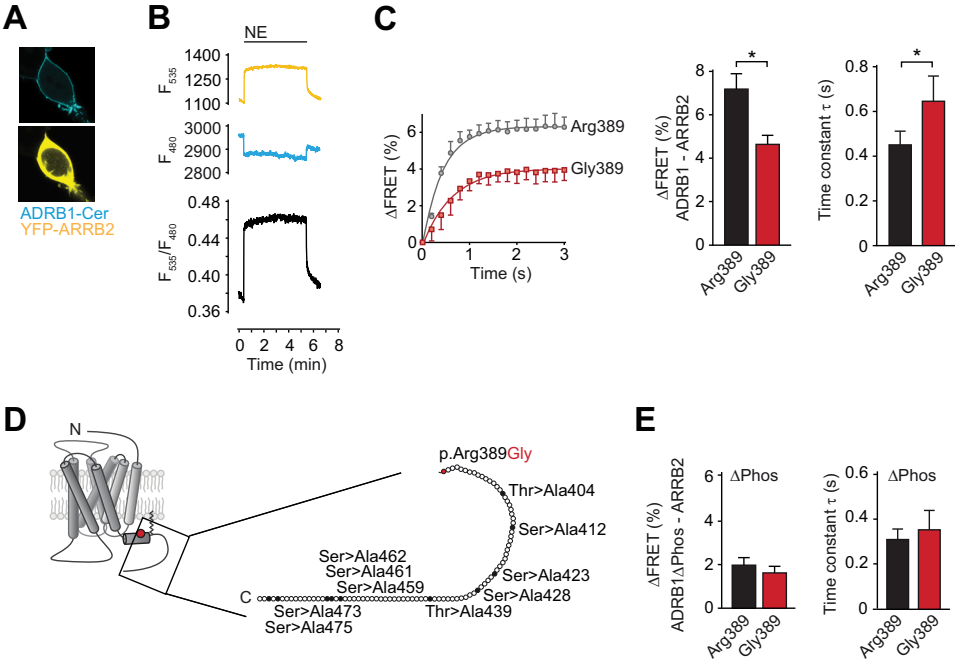

FIGURE 2. **The Arg-389 variant of the β_1-adrenoceptor is hyperfunctional with regard to agonist-dependent arrestin recruitment.** *A*, representative confocal images (×63) for cellular localization of the constructs after cotransfection in HEK293 cells (YFP fluorescence is depicted in *yellow* and Cer in *cyan*). *B*, FRET tracing monitoring the interaction of ADRB1-Cer and YFP-ARRB2. *C*, amplitude and time constant of the NE-induced change in FRET between YFP-ARRB2 and ADRB1-Cer ($n = 14–20$). *, $p < 0.05$; Student's *t* test. *D*, overview of putative C-terminal phosphorylation sites (serines and threonines) that were mutated to alanine in the ADRB1(ΔPhos)-Cer construct used for FRET measurements in *E*. *E*, amplitude and time constant of the NE-induced change in FRET between YFP-ARRB2 and ADRB1(ΔPhos)-Cer.

YFP and, hence, a decrease in the FRET ratio (YFP/Cer) (Fig. 3*B*). The activation profile, *i.e.* the speed and amplitude of ADRB1 activation upon receptor stimulation with a saturating concentration of NE, did not differ between the Arg-389 and Gly-389 variants at the first contact with the agonist. To simulate conditions that would more closely reflect receptor activation occurring *in vivo*, we subjected the receptor FRET sensor cells to repeated agonist activation (Fig. 3*B*). Under these conditions, Arg-389-ADRB1 displayed significantly faster activation kinetics than Gly-389-ADRB1. Compared with the initial stimulation, the latter became slower in its activation, whereas Arg389-ADRB1 retained its high activation speed (Fig. 3, *C* and *D*). The amplitude of the FRET signal, *i.e.* the decrease in FRET ratio, was not significantly different (Fig. 3*E*).

The Different Activation Kinetics of the ADRB1 Variants Are Dependent on Receptor Phosphorylation and the Interaction with Soluble Intracellular Proteins—The data shown so far suggested that activation of Arg-389-ADRB1 occurs faster than that of the Gly-389 variant and that this is due to hyperphosphorylation of the former. We next sought to elucidate whether phosphorylation of ADRB1 accounts for the difference in activation speed of the ADRB1 variants. Two approaches indicated that this is indeed the case. First, receptor activation FRET sensors for both variants in which the C-terminal putative ADRB1 phosphorylation sites had been mutated showed nearly identical activation kinetics (Fig. 4, *A* and *B*). Mutation of ten C-terminal serine/threonine residues did not compromise receptor functionality: The amplitude of the FRET signal was not altered compared with the wild-type sensors (Fig. 3*E*) (Arg-389ΔPhos sensor, 1.70 ± 0.10%; Gly-389ΔPhos sensor, 1.88 ± 0.24%). Furthermore, the efficacy of NE-mediated cAMP formation was unchanged (EC_{50} of the Arg-389 sensor, 419 ± 167 nM; EC_{50} of the Arg-389ΔPhos sensor, 232 ± 123 nM, EC_{50} of the Gly-389 sensor, 308 ± 77 nM; and EC_{50} of the Gly-389ΔPhos sensor, 354 ± 213 nM; $n = 4$). The differences in potency were blunted upon deletion of the putative C-terminal phosphorylation sites (Fig. 4*C*).

The variant-dependent difference in receptor activation was likewise abolished when the receptor-phosphorylating kinases GRK2, 3, 5, and 6 were silenced with siRNAs (Fig. 4*B*, *columns 5* and *6*). Additional evidence for the involvement of intracellular interactors was obtained by treatment of the HEK293 cells stably expressing the FRET sensors with the cell-permeabilizing agent saponin. Treatment with saponin was highly efficient because it led to a rapid efflux of diffusible intracellular factors, exemplified by RFP-tagged β-arrestin (Fig. 4*D*). Similar to the interference with receptor phosphorylation, deprivation of soluble intracellular factors abolished the variation-dependent differences in ADRB1 activation kinetics (Fig. 4*E*).

The Variants at Position 389 Determine Receptor Activation by Affecting Helix 1-Helix 8 Interaction—Next we addressed whether position 389 directly affects downstream signaling or whether its potential impact on the overall structure of the receptor would determine receptor efficacy. In an attempt to better understand the structural context of position 389, we performed homology modeling of human ADRB1 and based this on the structure of the carvedilol-bound turkey ADRB1 (PDB code 4AMJ) (17), where Arg-$355^{8.56}$ corresponds to Arg-389 in humans. The ADRB1 protein sequence of human and turkey are 64% identical with high conservation of the helices, including the region around Arg-389 in helix 8. Our model predicts that position 389 is located within helix 8 and that its

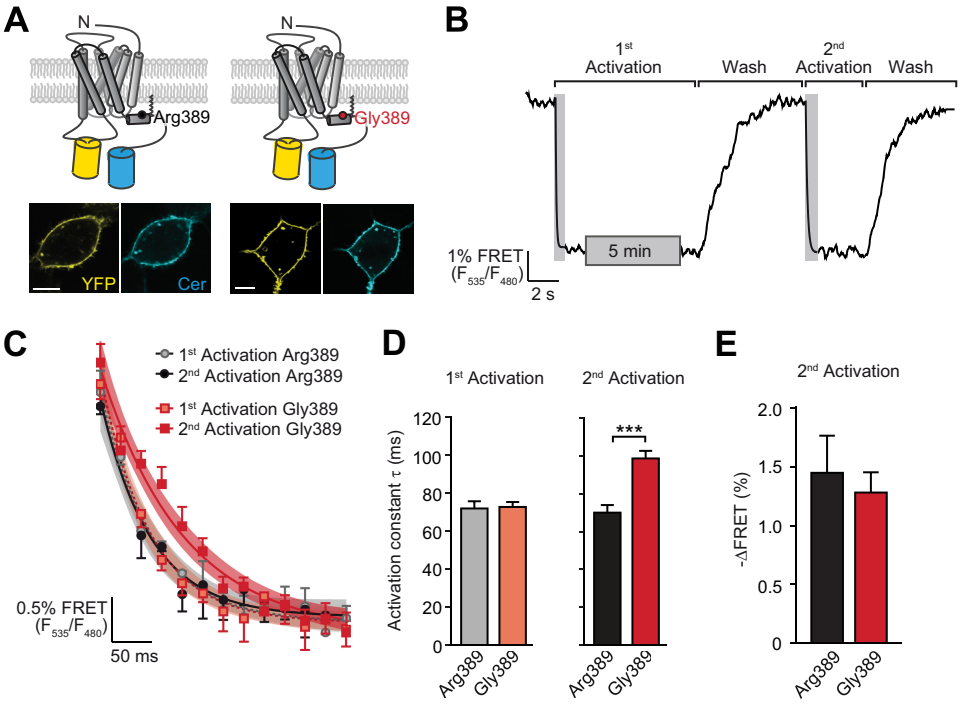

FIGURE 3. **The hyperfunctional Arg-389-ADRB1 exhibits faster activation compared with Gly389-ADRB1.** *A*, topology of the polymorphic ADRB1-FRET sensor constructs and their subcellular localization upon expression in HEK293 cells. *Scale bars* = 10 μm. YFP fluorescence is depicted in *yellow* and Cer in *cyan*. *B*, schematic of the experimental approach investigating ADRB1 activation kinetics upon repeated stimulation. *C*, activation kinetics of the ADRB1-FRET sensor variants Arg-389 and Gly-389 upon repeated stimulation with 100 μM NE. The first stimulation was carried out for 5 min and the second stimulation directly after complete washout of the agonist. Time constants were determined by fitting monoexponential curves to the first (*dashed line*) and second (*continuous line*) activation. Curves were fitted to plot the mean ± S.E. of the first and second activation ($n = 4–5$). 95% confidence intervals are displayed as *shaded areas*. *D*, time constants of the first (*left panel*) and second (*right panel*) activation ($n = 14–20$). ***, $p < 0.001$; Student's *t* test. *E*, FRET ratio of the second activation.

side chain is oriented toward helix 1 (Fig. 5*A*, *left panel*). Within helix 1, the side chains of Lys-85$^{1.59}$ and Thr-86$^{1.60}$ are in juxtaposition (Fig. 5*A*, *right panel*). Both amino acids comprise polar side chains that provide a basis for their putative interaction with the positively charged Arg-389. Although Thr-86$^{1.60}$ carries an OH group and, therefore, could interact with Arg-389 via hydrogen bonding, repulsion occurs between the guanidinium group of Arg-389 and the ϵ-amino group of Lys-85$^{1.59}$ in helix 1. The electrostatic interaction of both residues with position 389 is different in the Gly-389 variant.

These predictions prompted us to test the hypothesis that the interface between Arg-389 and helix 1 in human ADRB1 determines its activation kinetics and, hence, the differences observed between the two variants at position 389. Disrupting the interface of Arg-389 and helix 1 would then be predicted to result in a slower activation of the Arg-389 variant, similar to what is observed for Gly-389-ADRB1. To experimentally test this hypothesis, the respective residues in helix 1 were mutated in our FRET sensors for human ADRB1 (Lys-85 → Leu-85/Thr-86 → Val-86) (Fig. 5*B*). The activation profile of the ADRB1 sensors mutated in helix 1 was highly similar to the wild-type variants with regard to the first stimulation with NE (Fig. 5*C*). However, both the mutated Arg-389 and Gly-389 variants displayed slower and nearly identical activation kinetics upon repeated stimulation (Fig. 5*D*). Exchange of Lys-85/Thr-86 to Leu-85/Val-86 in helix 1 furthermore abolished the higher efficacy of the Arg-389 variant (Fig. 5, *E* and *F*). Mutation of residues 85 and 86 within helix 1 therefore specifically impaired the activation of the hyperfunctional Arg-389 variant (but not that of the Gly-389 variant), suggesting that the interface between helices 1 and 8 in the ADRB1 protein is critical for receptor activation and downstream signaling of Arg-389-ADRB1.

DISCUSSION

G protein-coupled receptors display considerable genetic variation. For several GPCRs, functional relevance of amino acid-changing variations has been described. One of the most intensely studied GPCR variants with regard to its effect on cellular signaling and its role in physiology and disease is the c.1165C>G (p.Arg389Gly) variation in the human β_1-adrenoceptor (4). In comparison to the Gly-389 variant, Arg-389-ADRB1 has been shown to exert higher efficacy for cAMP formation and a stronger response to β-agonists and β-antagonists. The mechanistic basis for this difference has remained elusive to date.

Here we show that agonist-dependent phosphorylation and subsequent recruitment of β-arrestin 2 is increased for the Arg-389 variant compared with Gly-389-ADRB1. Under simulated *in vivo* conditions (*i.e.* upon repeated stimulation), Arg-389-ADRB1 displayed faster activation kinetics, a finding that was dependent on receptor phosphorylation. Homology modeling followed by site-directed mutagenesis of human ADRB1 revealed that the interface of the side chain of Arg-389 and opposing amino acid residues in helix 1 determines its higher activation speed.

Hyperfunctionality of Arg-389-ADRB1 was first described with regard to agonist-stimulated adenylyl cylase activation determined in membrane preparations (5), a finding that was

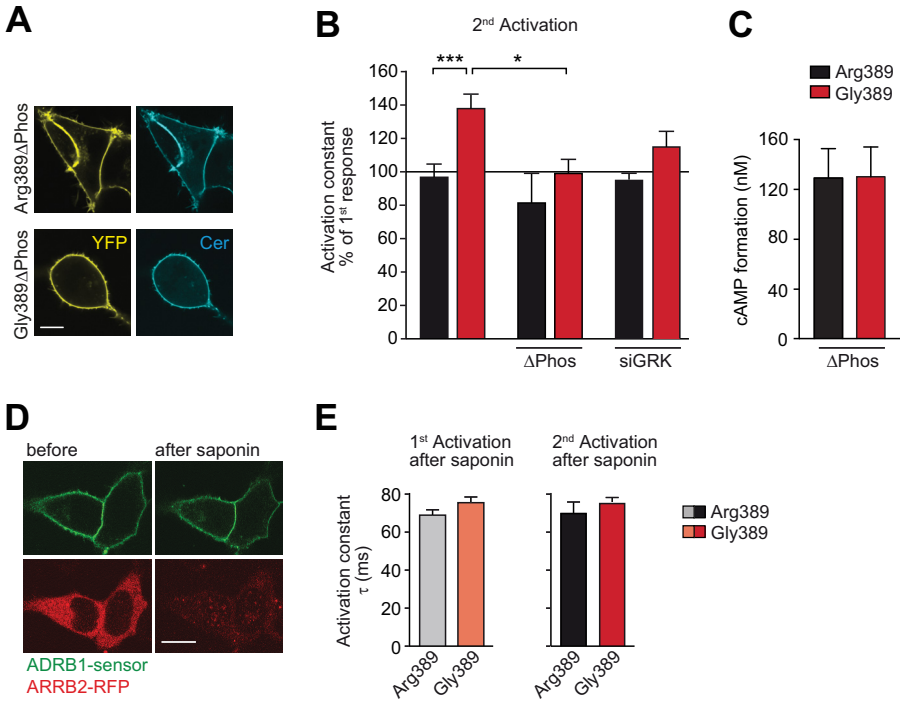

FIGURE 4. **The interaction of the activated ADRB1 with soluble intracellular proteins and ADRB1 phosphorylation is indispensable for variation-specific activation kinetics.** *A*, cellular localization of the phosphorylation-deficient ADRB1 sensor mutants (Δ*Phos*). *Scale bar* = 10 μm. The mutations introduced to delete putative C-terminal phosphorylation sites are shown in Fig. 2*D*. *B*, activation kinetics without further intervention (data from Fig. 3*D*) upon mutation of C-terminal phosphorylation sites (Δ*Phos*) or cotransfection of an siRNA mixture targeting GRK-2, 3, 5, and 6 (n = 5–7). *, $p < 0.05$; ***, $p < 0.001$; two-way analysis of variance followed by Bonferroni post test. *C*, cAMP formation in HEK293 cells stably expressing the ΔPhos-ADRB1 sensor variants at comparable levels (Arg-389, 1.55 ± 0.22 pmol/mg; Gly-389, 1.49 ± 0.05 pmol/mg membrane protein; n = 3). Stimulation was carried out for 10 min with 1 μM NE in 384 wells containing 10,000 cells. *D*, qualitative control of saponin treatment. HEK293 cells expressing an ADRB1 FRET sensor at the plasma membrane and RFP-tagged β-arrestin 2 (*ARRB2-RFP*) in the cytosol before and after cell permeabilization with saponin for 3 min. *Scale bar* = 10 μm. *E*, activation kinetics of the ADRB1 sensors upon permeabilization-induced deprivation of intracellular proteins (n = 5). As in Fig. 3, the first stimulation was carried out for 5 min and the second stimulation directly after complete washout of the agonist.

corroborated by determinations of agonist-induced cAMP formation in whole cells. Mason *et al.* (5) reported enhanced G protein activation through Arg-389-ADRB1 as determined by GTPγS-binding. These data were obtained in membranes upon overexpression of $G_s\alpha$ and very high levels of receptor protein (approximately 10 pmol/mg membrane protein) and are therefore difficult to compare with most other experimental settings that have been applied for the investigation of receptor activation and signaling (7–9). Using FRET-based assays in living HEK293 cells, Rochais *et al.* (9) have reported a similar extent of G protein activation and cAMP formation through Gly-389-ADRB1 and Arg-389-ADRB1 upon a single exposure of the cells to norepinephrine. The latter findings are in good agreement with our notion that the two variants at position 389 behave similarly upon initial activation (and, hence, before phosphorylation-mediated modification of the receptor occurs). The prestimulated and therefore phosphorylated ADRB1 changed its activation kinetics in dependence of the variation p.Arg389Gly in helix 8. Arg-389-ADRB1 retained its initial speed of activation, and the Gly-389 variant became slower when activated repeatedly. We envision the following scenarios of how the faster activation of the Arg-389 variant may result in an increased efficacy (*i.e.* enhanced cAMP formation) compared with Gly-389-ADRB1. When norepinephrine binds to ADRB1, a larger fraction of the Arg-389 variant might assume an active state than it is the case for the Gly389-variant. However, this scenario seems unlikely because the FRET responses of the two variants are similar. Rather, we assume that the active and/or the inactive conformations of the two variants exert a difference that is not readily detectable with our FRET sensors for receptor activation.

Despite its hyperfunctionality, our data demonstrate that the Arg-389 variant is hyperphosphorylated (and likely recruits more β-arrestin) and that this is necessary to maintain its high speed of activation in comparison with the slower Gly-389. Although receptor phosphorylation has traditionally been regarded mainly as an initiating step of receptor desensitization, our data support the recently proposed concept that phosphorylation may determine receptor efficacy through the stabilization of distinct receptor conformations (18) and that β-arrestin recruitment of GPCRs initiates alternative routes of cellular signaling (19–21). Our finding of enhanced β-arrestin recruitment through Arg-389 is in good agreement with a recent study on this variant that reported enhanced MAPK signaling through Arg-389 (8), a signal that is generally assumed to depend on β-arrestin.

The hyperfunctional Arg-389 variant recruits arrestin more efficiently with regard to Gly-389-ADRB1, with arrestin constituting a major component of the GPCR desensitization machinery (particularly studied in great detail for the β_2-adrenoceptor (22)). However, norepinephrine-mediated arrestin binding to ADRB1 seems to be weak, and the desensitization process appears to be different for ADRB1 compared with ADRB2 (13), resulting in less internalization and down-regulation of ADRB1 (23, 24). Furthermore, we assume that, in our

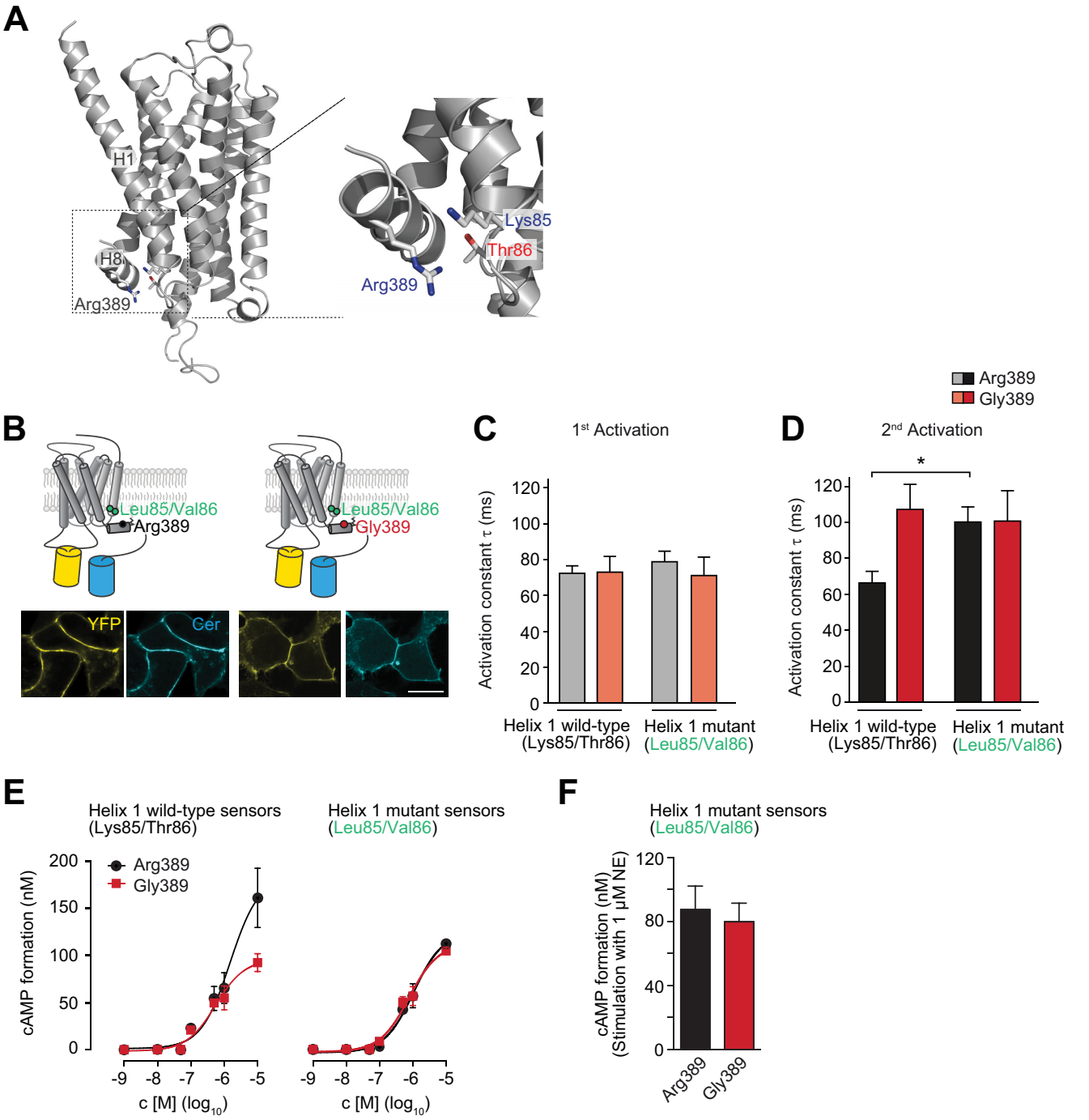

FIGURE 5. **The variant-specific interface of helices 1 and 8 is critical for ADRB1 activation kinetics.** *A*, model of the human ADRB1 protein on the basis of the resolved structure of the turkey ADRB1 bound to carvedilol (17) (generated using Prime, Schrödinger, LLC). Specifically, Arg-389 in helix 8 as well as Lys-85 and Thr-86 at the intracellular end of helix 1 are shown. *B*, cellular localization of the helix1-ADRB1 sensor mutants (Leu-85/Val-86-ADRB1). *Scale bar* = 10 μm. YFP fluorescence is depicted in *yellow* and Cer in *cyan*. *C* and *D*, time constants of (*C*) first and (*D*) second activation for the helix1-ADRB1 sensor mutants of the Arg-389 and Gly-389 variants ($n = 6-8$) and respective wild-type sensors ($n = 5-8$). The first stimulation was carried out for 5 min and the second stimulation directly after complete washout of the agonist. *, $p < 0.05$, Kruskal-Wallis test followed by Dunn's post test. *E*, representative concentration-response curve for cAMP formation in HEK293 cells stably expressing the Arg-389-ADRB1 sensor variants (Arg-389, 1.10 ± 0.15 pmol/mg; Gly-389, 1.13 ± 0.13 pmol/mg membrane protein; $n = 3$) and the helix 1 mutant sensors (Arg-389, 0.57 ± 0.11 pmol/mg; Gly-389, 0.63 ± 0.11 pmol/mg membrane protein; $n = 3$). *F*, cAMP formation in HEK293 cells stably expressing the helix 1 mutant sensor variants at comparable levels. Stimulation was carried out for 10 min with 1 μM NE in 384 wells containing 10,000 cells.

experimental setting for determination of cAMP formation (Fig. 1*A*), not every receptor is bound to arrestin at any point of time as we overexpress the ADRB1 variants, whereas only the endogenous arrestin pool is available.

We finally propose a mechanism underlying the observed differences in receptor activation and signaling. Homology modeling and site-directed mutagenesis suggest that the receptor conformation around arginine at position 389 in helix 8 is influenced by the Arg-389-opposing residues Lys-85 and Thr-86 at the intracellular end of transmembrane helix 1. The electrostatic interaction of Arg-389 might aid the receptor to return to an inactive conformation, which is different from the

inactive conformation of the prestimulated Gly-389-ADRB1. Starting from the inactive conformation of the prestimulated Arg-389-ADRB1, activation is faster and, therefore, allows this variant to retain its initial speed of activation.

Because the disturbance of the Arg-389-helix 1 interface slowed activation of the Arg-389 variant, we hypothesize that the helix 8-helix 1 interface directly determines variant-specific receptor conformation of the phosphorylated receptor. Accordingly, the two variants of the receptor need to assume different conformations, although these different "basal" conformations are not amenable to our sensor approach. NMR spectroscopy and molecular dynamics simulations that were made on the basis of structure determination of antagonist- and agonist-bound and G protein-coupled states of the same GPCR predict that a GPCR assumes multiple conformations and oscillates between them (25, 26). In this concept, a certain "state" of a GPCR (*e.g.* bound to a specific ligand) merely occurs with a certain likelihood. Future studies can be expected to increase the number of defined conformations of individual GPCRs as well as our understanding of the dynamic transitions between them. Such work may also include receptor variation and posttranslational modifications such as receptor phosphorylation.

A future step with regard to the variation of ADRB1 would be the crystallization of the human ADRB1 variants at position 389 both in the active and inactive states. Delineation of the conformation of the C terminus is challenging because it appears highly dynamic and is not structured. The C terminus has not been solved for any GPCR to date (17, 27–31). This would show whether the differential phosphorylation is a quantitative effect or whether the accessibility of residues for phosphorylation by GRKs is altered because of variant-specific conformation of the C terminus. The latter may involve a phosphorylation "bar code" for ADRB1 variants, a phenomenon that has been described for the β_2-adrenoceptor upon binding of different ligands (16) and for the M3 muscarinic receptor upon activation in different cell types (32). Studies on β_1-adrenoceptor phosphorylation published to date focus on whole receptor phosphorylation by protein kinase A or GRKs (19, 23, 24, 33) but did not investigate specific phosphorylation sites. It appears conceivable that the variant-specific conformation of ADRB1 determines the pattern of its phosphorylation and that this determines receptor efficacy through the stabilization of certain receptor conformations.

Acknowledgments—We thank J. Valcourt (D. E. Shaw Research, New York, NY) and R. O. Dror (D.E. Shaw Research and Institute of Computational and Mathematical Engineering, Stanford University, Stanford, CA) for the model of the human β_1-adrenoceptor and M. Ungerer (advanceCor GmbH, Martinsried, Germany) for the anti-ADRB1 antibody. We also thank C. Dees (Institute of Pharmacology and Toxicology, Universität Würzburg, Würzburg, Germany) for help and advice with regard to radioligand-binding assays, M. Brill and T. Misgeld (Institute of Neuroscience, Technische Universität München, Munich, Germany) for confocal microscopy support, and M. J. Lohse (Institute of Pharmacology and Toxicology, Universität Würzburg) for critical discussion of the data.

REFERENCES

1. Kirstein, S. L., and Insel, P. A. (2004) Autonomic nervous system pharmacogenomics: a progress report. *Pharmacol. Rev.* **56,** 31–52
2. Lymperopoulos, A., Rengo, G., and Koch, W. J. (2013) Adrenergic nervous system in heart failure: pathophysiology and therapy. *Circ. Res.* **113,** 739–753
3. Rosskopf, D., and Michel, M. C. (2008) Pharmacogenomics of G protein-coupled receptor ligands in cardiovascular medicine. *Pharmacol. Rev.* **60,** 513–535
4. Ahles, A., and Engelhardt, S. (2014) Polymorphic variants of adrenoceptors: pharmacology, physiology, and role in disease. *Pharmacol. Rev.* **66,** 598–637
5. Mason, D. A., Moore, J. D., Green, S. A., and Liggett, S. B. (1999) A gain-of-function polymorphism in a G-protein coupling domain of the human β1-adrenergic receptor. *J. Biol. Chem.* **274,** 12670–12674
6. Tesson, F., Charron, P., Peuchmaurd, M., Nicaud, V., Cambien, F., Tiret, L., Poirier, O., Desnos, M., Jullières, Y., Amouyel, P., Roizès, G., Dorent, R., Schwartz, K., and Komajda, M. (1999) Characterization of a unique genetic variant in the β1-adrenoceptor gene and evaluation of its role in idiopathic dilated cardiomyopathy: CARDIGENE Group. *J. Mol. Cell Cardiol.* **31,** 1025–1032
7. Joseph, S. S., Lynham, J. A., Grace, A. A., Colledge, W. H., and Kaumann, A. J. (2004) Markedly reduced effects of (−)-isoprenaline but not of (−)-CGP12177 and unchanged affinity of β-blockers at Gly389-β1-adrenoceptors compared to Arg389-β1-adrenoceptors. *Br. J. Pharmacol.* **142,** 51–56
8. Zhang, F., and Steinberg, S. F. (2013) S49G and R389G polymorphisms of the β1-adrenergic receptor influence signaling via the cAMP-PKA and ERK pathways. *Physiol. Genomics* **45,** 1186–1192
9. Rochais, F., Vilardaga, J. P., Nikolaev, V. O., Bünemann, M., Lohse, M. J., and Engelhardt, S. (2007) Real-time optical recording of β1-adrenergic receptor activation reveals supersensitivity of the Arg389 variant to carvedilol. *J. Clin. Invest.* **117,** 229–235
10. Tikhonoff, V., Hasenkamp, S., Kuznetsova, T., Thijs, L., Jin, Y., Richart, T., Zhang, H., Brand-Herrmann, S.-M., Brand, E., Casiglia, E., and Staessen, J. (2008) Blood pressure and metabolic phenotypes in relation to the ADRB1 Arg389Gly and ADRA2B I/D polymorphisms in a White population. *J. Hum. Hypertens.* **22,** 864–867
11. Gjesing, A. P., Andersen, G., Albrechtsen, A., Glümer, C., Borch-Johnsen, K., Jørgensen, T., Hansen, T., and Pedersen, O. (2007) Studies of associations between the Arg389Gly polymorphism of the β1-adrenergic receptor gene (ADRB1) and hypertension and obesity in 7677 Danish white subjects. *Diabet. Med.* **24,** 392–397
12. Johnson, A. D., Newton-Cheh, C., Chasman, D. I., Ehret, G. B., Johnson, T., Rose, L., Rice, K., Verwoert, G. C., Launer, L. J., Gudnason, V., Larson, M. G., Chakravarti, A., Psaty, B. M., Caulfield, M., van Duijn, C. M., Ridker, P. M., Munroe, P. B., and Levy, D. (2011) Association of hypertension drug target genes with blood pressure and hypertension in 86,588 individuals. *Hypertension* **57,** 903–910
13. Ahles, A., Rochais, F., Frambach, T., Bünemann, M., and Engelhardt, S. (2011) A polymorphism-specific "memory" mechanism in the β(2)-adrenergic receptor. *Sci. Signal.* **4,** ra53
14. Vilardaga, J.-P., Bünemann, M., Krasel, C., Castro, M., and Lohse, M. J. (2003) Measurement of the millisecond activation switch of G protein-coupled receptors in living cells. *Nat. Biotechnol.* **21,** 807–812
15. Lohse, M. J., Nuber, S., and Hoffmann, C. (2012) Fluorescence/bioluminescence resonance energy transfer techniques to study G-protein-coupled. *Pharmacol. Rev.* **64,** 299–336
16. Nobles, K. N., Xiao, K., Ahn, S., Shukla, A. K., Lam, C. M., Rajagopal, S., Strachan, R. T., Huang, T.-Y., Bressler, E. A., Hara, M. R., Shenoy, S. K., Gygi, S. P., and Lefkowitz, R. J. (2011) Distinct phosphorylation sites on the β(2)-adrenergic receptor establish a barcode that encodes differential functions of β-arrestin. *Sci. Signal.* **4,** ra51
17. Warne, T., Edwards, P. C., Leslie, A. G., and Tate, C. G. (2012) Crystal structures of a stabilized β1-adrenoceptor bound to the biased agonists bucindolol and carvedilol. *Structure* **20,** 841–849
18. Kenakin, T. (2013) New concepts in pharmacological efficacy at 7TM

receptors: IUPHAR review 2. *Br. J. Pharmacol.* **168,** 554–575
19. Noma, T., Lemaire, A., Naga Prasad, S. V., Barki-Harrington, L., Tilley, D. G., Chen, J., Le Corvoisier, P., Violin, J. D., Wei, H., Lefkowitz, R. J., and Rockman, H. A. (2007) β-Arrestin-mediated beta1-adrenergic receptor transactivation of the EGFR confers cardioprotection. *J. Clin. Invest.* **117,** 2445–2458
20. Tilley, D. G., Kim, I.-M., Patel, P. A., Violin, J. D., and Rockman, H. A. (2009) β-Arrestin mediates β1-adrenergic receptor-epidermal growth factor receptor interaction and downstream signaling. *J. Biol. Chem.* **284,** 20375–20386
21. Kim, I.-M., Wang, Y., Park, K.-M., Tang, Y., Teoh, J.-P., Vinson, J., Traynham, C. J., Pironti, G., Mao, L., Su, H., Johnson, J. A., Koch, W. J., and Rockman, H. A. (2014) β-Arrestin1-biased β1-Adrenergic receptor signaling regulates microRNA processing. *Circ. Res.* **114,** 833–844
22. Perry, S. J., Baillie, G. S., Kohout, T. A., McPhee, I., Magiera, M. M., Ang, K. L., Miller, W. E., McLean, A. J., Conti, M., Houslay, M. D., and Lefkowitz, R. J. (2002) Targeting of cyclic AMP degradation to β 2-adrenergic receptors by β-arrestins. *Science* **298,** 834–836
23. Liang, W., Austin, S., Hoang, Q., and Fishman, P. H. (2003) Resistance of the human β 1-adrenergic receptor to agonist-mediated down-regulation: role of the C terminus in determining β-subtype degradation. *J. Biol. Chem.* **278,** 39773–39781
24. Rapacciuolo, A., Suvarna, S., Barki-Harrington, L., Luttrell, L. M., Cong, M., Lefkowitz, R. J., and Rockman, H. A. (2003) Protein kinase A and G protein-coupled receptor kinase phosphorylation mediates β-1 adrenergic receptor endocytosis through different pathways. *J. Biol. Chem.* **278,** 35403–35411
25. Dror, R. O., Arlow, D. H., Maragakis, P., Mildorf, T. J., Pan, A. C., Xu, H., Borhani, D. W., and Shaw, D. E. (2011) Activation mechanism of the β2-adrenergic receptor. *Proc. Natl. Acad. Sci. U.S.A.* **108,** 18684–18689
26. Nygaard, R., Zou, Y., Dror, R. O., Mildorf, T. J., Arlow, D. H., Manglik, A., Pan, A. C., Liu, C. W., Fung, J. J., Bokoch, M. P., Thian, F. S., Kobilka, T. S., Shaw, D. E., Mueller, L., Prosser, R. S., and Kobilka, B. K. (2013) The dynamic process of β(2)-adrenergic receptor activation. *Cell* **152,** 532–542
27. Warne, T., Serrano-Vega, M. J., Baker, J. G., Moukhametzianov, R., Edwards, P. C., Henderson, R., Leslie, A. G., Tate, C. G., and Schertler, G. F. (2008) Structure of a β1-adrenergic G-protein-coupled receptor. *Nature* **454,** 486–491
28. Warne, T., Moukhametzianov, R., Baker, J. G., Nehmé, R., Edwards, P. C., Leslie, A. G., Schertler, G. F., and Tate, C. G. (2011) The structural basis for agonist and partial agonist action on a β(1)-adrenergic receptor. *Nature* **469,** 241–244
29. Rasmussen, S. G., Choi, H.-J., Rosenbaum, D. M., Kobilka, T. S., Thian, F. S., Edwards, P. C., Burghammer, M., Ratnala, V. R., Sanishvili, R., Fischetti, R. F., Schertler, G. F., Weis, W. I., and Kobilka, B. K. (2007) Crystal structure of the human β2 adrenergic G-protein-coupled receptor. *Nature* **450,** 383–387
30. Rasmussen, S. G., DeVree, B. T., Zou, Y., Kruse, A. C., Chung, K. Y., Kobilka, T. S., Thian, F. S., Chae, P. S., Pardon, E., Calinski, D., Mathiesen, J. M., Shah, S. T., Lyons, J. A., Caffrey, M., Gellman, S. H., Steyaert, J., Skiniotis, G., Weis, W. I., Sunahara, R. K., and Kobilka, B. K. (2011) Crystal structure of the β2 adrenergic receptor-Gs protein complex. *Nature* **477,** 549–555
31. Ring, A. M., Manglik, A., Kruse, A. C., Enos, M. D., Weis, W. I., Garcia, K. C., and Kobilka, B. K. (2013) Adrenaline-activated structure of β2-adrenoceptor stabilized by an engineered nanobody. *Nature* **502,** 575–579
32. Tobin, A. B., Butcher, A. J., and Kong, K. C. (2008) Location, location, location: site-specific GPCR phosphorylation offers a mechanism for cell-type-specific signalling. *Trends Pharmacol. Sci.* **29,** 413–420
33. Freedman, N. J., Liggett, S. B., Drachman, D. E., Pei, G., Caron, M. G., and Lefkowitz, R. J. (1995) Phosphorylation and desensitization of the human β 1-adrenergic receptor: involvement of G protein-coupled receptor kinases and cAMP-dependent protein kinase. *J. Biol. Chem.* **270,** 17953–17961
34. Cheng, Y., and Prusoff, W. H. (1973) Relationship between the inhibition constant (K_I) and the concentration of inhibitor which causes 50 per cent inhibition (I_{50}) of an enzymatic reaction. *Biochem. Pharmacol.* **22,** 3099–3108.